REPORT DOCUMENTATION PAGE

Form Approved OMB NO. 0704-0188

1. REPORT DATE (DD-MM-YYYY)	2. REPORT TYPE	3. DATES COVERED (From - To)
08-08-2022	Final Report	15-Feb-2018 - 14-Oct-2021

4. TITLE AND SUBTITLE
Final Report: Vaporization, Mixing, and Ignition Dynamics in High-Pressure Evaporating and Reacting Sprays

5a. CONTRACT NUMBER
W911NF-18-1-0086

5b. GRANT NUMBER

5c. PROGRAM ELEMENT NUMBER
611102

6. AUTHORS

5d. PROJECT NUMBER

5e. TASK NUMBER

5f. WORK UNIT NUMBER

7. PERFORMING ORGANIZATION NAMES AND ADDRESSES
Ohio State University
1960 Kenny Road

Columbus, OH 43210 -1016

8. PERFORMING ORGANIZATION REPORT NUMBER

9. SPONSORING/MONITORING AGENCY NAME(S) AND ADDRESS (ES)
U.S. Army Research Office
P.O. Box 12211
Research Triangle Park, NC 27709-2211

10. SPONSOR/MONITOR'S ACRONYM(S)
ARO

11. SPONSOR/MONITOR'S REPORT NUMBER(S)
72584-EG.5

12. DISTRIBUTION AVAILIBILITY STATEMENT
Approved for public release; distribution is unlimited.

13. SUPPLEMENTARY NOTES
The views, opinions and/or findings contained in this report are those of the author(s) and should not contrued as an official Department of the Army position, policy or decision, unless so designated by other documentation.

14. ABSTRACT

15. SUBJECT TERMS

16. SECURITY CLASSIFICATION OF:			17. LIMITATION OF ABSTRACT	15. NUMBER OF PAGES	19a. NAME OF RESPONSIBLE PERSON
a. REPORT	b. ABSTRACT	c. THIS PAGE			Jeffrey Sutton
UU	UU	UU	UU		19b. TELEPHONE NUMBER 614-688-4999

RPPR Final Report
as of 11-Aug-2022

Agency Code: 21XD

Proposal Number: 72584EG **Agreement Number: W911NF-18-1-0086**
INVESTIGATOR(S):

Name: Jeffrey A Sutton
Email: sutton.235@osu.edu
Phone Number: 6146884999
Principal: Y

Organization: **Ohio State University**
Address: 1960 Kenny Road, Columbus, OH 432101016
Country: USA

DUNS Number: 832127323 EIN: 316025986
Report Date: 14-Jan-2022 Date Received: 08-Aug-2022
Final Report for Period Beginning 15-Feb-2018 and Ending 14-Oct-2021
Title: Vaporization, Mixing, and Ignition Dynamics in High-Pressure Evaporating and Reacting Sprays
Begin Performance Period: 15-Feb-2018 **End Performance Period:** 14-Oct-2021
Report Term: 0-Other

Submitted By: Jeffrey Sutton Email: sutton.235@osu.edu
Phone: (614) 688-4999

Distribution Statement: 1-Approved for public release; distribution is unlimited.

STEM Degrees: 0 **STEM Participants:** 3

Major Goals: The objective of the proposed research is to investigate vaporization, gas-phase mixing, and ignition dynamics in evaporating (non-reacting) and reacting sprays at high pressures and high temperatures. State-of-the art optical and laser-based diagnostics are targeted for (i) characterizing the effects of injection (pressure, mass, and duration) and operating conditions (ambient pressure and temperature) on gas-phase mixing topology, (ii) examining CH2O (low-temperature species) concentration fields, the correlation with the liquid spray and gas-phase mixing topology, and the dependence on injection and operating conditions, and (iii) providing new information regarding the role of low-temperature (first-stage) ignition and mixing dynamics on the onset high-temperature ignition. A major target is the measurement of a series of conditional statistics that detail the most probable mixture composition for facilitating ignition and the correlation between low-temperature species such as CH2O and the onset of high-temperature, second-stage ignition. A research objective that manifested itself after the project initiation was the construction and implementation of a new, high-pressure, high-temperature spray and ignition facility that would greatly benefit the current and future research programs. Furthermore, additional measurements in an atmospheric ignition experiment were added to elucidate the fundamental roles of mixing and fluid turbulence on ignition kernel formation.

Some fundamental questions to be answered include:
(i) Where does vaporization occur in relation to the liquid spray plume, i.e., what is the correlation between fuel vapor (and vapor-ambient mixtures) and liquid droplet position? How does this change as a function of liquid mass injection and ambient density?
(ii) When (time following fuel injection) and where (with respect to the liquid spray plume) do lower-temperature species such as CH2O form? What fuel vapor conditions are highly correlated with CH2O formation?
(iii) What is the spatial structure of the CH2O field following fuel injection and how does it evolve during the induction period leading to second-stage ignition? What is the correlation between the local CH2O fluctuations and the equivalence ratio field?
(iv) When and where (spatial location) does second-stage ignition occur? What are the most probable mixing (local equivalence ratio) conditions supporting “hot” ignition?
(v) Does high-temperature ignition occur in regions of high CH2O concentrations (i.e., regions of fuel pyrolysis and partial oxidation) or regions with high CH2O gradients, indicating an importance in species transport and cool flame propagation?

Accomplishments: This information is supplied in the uploaded document.

RPPR Final Report
as of 11-Aug-2022

Training Opportunities: As part of this project, one graduate student was fully supported as well as one partially supported post-doctoral researcher. In addition, two other graduate students and one post-doc worked on this project. Within the project, training activities for the graduate students included one-on-one training with the PI and a post-doctoral researchers. Individual time was spent onsite within the laboratory teaching fundamental aspects of laser diagnostics and experimentation. Additional training consisted of an advanced course in "optical diagnostics in fluid flows". This course was taught in the spring semester of 2018 at OSU and was attended by the three graduate students. The graduate students learned about several cutting-edge technology as part of their training, including advanced engine/propulsion systems and advanced optical/laser diagnostics. One supported graduate student and one post-doctoral research spent significant time designing and constructing a new high-pressure facility. This experience is almost unprecedented within academia. Overall, the students will graduate with a significant skill set - one that makes them highly desired within the scientific community. By being introduced to DoD applications and research problems during the course of this project, the students will be poised to make contributions to DoD laboratories and research issues upon graduation. The post-doctoral researchers have had opportunities to oversee a portion of the technical work and assist in advising the supported graduate students. This is invaluable training for the post-docs who are in a critical portion of their careers (between student and senior-level researcher). Due to Covid19, many professional development opportunities, including travel to conferences and workshops, have not been possible. However, papers based on the research were submitted to conferences by the students and post-doc.

Results Dissemination: In terms of publications and presentations, two conference papers were submitted and accepted to AIAA Scitech conference. These papers were presented (virtually) by the students. To date, two journal papers have been published - AIAA Journal and the Proceedings of the Combustion Institute. It is expected that several more papers will result from this project as the acquired data is still being processed. We also have given a presentation at the Engine Combustion Network (ECN) teleconference describing our new facility, its capabilities, and preliminary results. A supported graduate student gave the presentation, which was well received by an international community of researchers and scholars.

We have collaborated with several DoD researchers at both AFRL and NRL. While this collaborations were not directly with Army researchers, the scientific methods were eventually adapted to this project.

Honors and Awards: • The PI [Sutton] was elected to Editorial Board, Combustion and Flame, 2018
• The PI [Sutton] was elected to the Program Advisory Committee, 38th International Symposium on Combustion, 2018
• The PI [Sutton] was selected as Colloquium Chair, 38th International Symposium on Combustion, 2019
• The PI [Sutton] and graduate student were selected for a Best Paper Award, AIAA, Aerodynamic Measurement Technology, 2019
• The PI [Sutton] and graduate student's paper was selected as Editor's Pick, 2019
• The PI [Sutton] was promoted to full Professor at OSU, 2019

Protocol Activity Status:

Technology Transfer: The primary technology transfer during this project occurred in the form of interactions with DoD laboratories. In 2018, we began planning with Drs. Campbell Carter and Steven Hammack from AFRL for time-resolved, volumetric measurements of the CH2O intermediate in turbulent premixed flames. The 4D measurements were to be performed using the uniquehigh-energy pulse burst laser system at OSU. A secondary target of the measurements were to serve as proof-of-concept for potential time-resolved, volumetric CH2O measurements within a high-pressure spray environment (current program). In 2019, we collaborated with Drs. Campbell Carter and Steven Hammack from AFRL on applying our newly developed wavelet-based optical flow velocimetry (wOFV) for high-resolution, velocimetry measurements in turbulent premixed flames. This collaboration resulted in a presentation at the International Symposium on Combustion and publication within the Proceedings of the Combustion Institute. In 2021, we began collaborating with Drs. Cambell Carter and Steven Hammack of AFRL; Dr. Steven Tuttle of NRL, and Drs. Scott Peltier, Brian Rice, and Tom McManus of AFRL on high-speed boundary layer measurements. In addition to these established and executed collaborations, there were additional preliminary discussions with Army Research Lab personnel concerning collaborations that did not materialize, primarily to the COVID pandemic.

PARTICIPANTS:

RPPR Final Report
as of 11-Aug-2022

Participant Type: PD/PI
Participant: JEFFREY Alan SUTTON
Person Months Worked: 3.00 **Funding Support:**
Project Contribution:
National Academy Member: N

Participant Type: Postdoctoral (scholar, fellow or other postdoctoral position)
Participant: Wesley Boyette
Person Months Worked: 6.00 **Funding Support:**
Project Contribution:
National Academy Member: N

Participant Type: Graduate Student (research assistant)
Participant: Jeremy Manus
Person Months Worked: 6.00 **Funding Support:**
Project Contribution:
National Academy Member: N

Participant Type: Postdoctoral (scholar, fellow or other postdoctoral position)
Participant: Bryan Schmidt
Person Months Worked: 3.00 **Funding Support:**
Project Contribution:
National Academy Member: N

Participant Type: Graduate Student (research assistant)
Participant: Ignacio Trueba-Monje
Person Months Worked: 2.00 **Funding Support:**
Project Contribution:
National Academy Member: N

Participant Type: Graduate Student (research assistant)
Participant: Sean Yan
Person Months Worked: 1.00 **Funding Support:**
Project Contribution:
National Academy Member: N

ARTICLES:

RPPR Final Report
as of 11-Aug-2022

Publication Type: Journal Article Peer Reviewed: Y **Publication Status:** 1-Published
Journal: AIAA Journal
Publication Identifier Type: DOI Publication Identifier: 10.2514/1.J060819
Volume: 60 Issue: 4 First Page #: 1
Date Submitted: 8/2/22 12:00AM Date Published: 4/1/22 4:00AM
Publication Location:
Article Title: On the Application of the Abel Transformation in Statistically Axisymmetric Turbulent Flows
Authors: Bryan Schmidt, Wayne Page, Jeffrey Sutton
Keywords: Abel Transformation, turbulent flows, optical flow
Abstract: The application of the inverse Abel transformation to statistically axisymmetric data is described in this work. The general theory of Abel inversion tomography is discussed, and it is shown that in order to properly apply the Abel inversion, an ensemble operator must be axisymmetric and commute with path integration. For statistically axisymmetric data where the individual realizations are asymmetric (such as turbulent flows issuing from circular nozzles), only the planar mean can be properly recovered. Higher-order moments, such as the standard deviation (root mean square) cannot be recovered because path integration is not commutative with the statistical moment operators. It is further shown that the Abel transformation cannot be used to recover the one-sided Fourier spectrum for the same reason. For the mean, the Abel inversion can be applied to the ensemble quantity, or the ensemble operator can be applied to the Abel inversion of individual asymmetric realizations.
Distribution Statement: 1-Approved for public release; distribution is unlimited.
Acknowledged Federal Support: **Y**

Publication Type: Journal Article Peer Reviewed: Y **Publication Status:** 3-Accepted
Journal: Proceedings of the Combustion Institute
Publication Identifier Type: Publication Identifier:
Volume: Issue: First Page #:
Date Submitted: 8/2/22 12:00AM Date Published:
Publication Location:
Article Title: Experimental Determination of the Most Probable Mixing States for Auto-Ignition of Transient Fuel Injection into Hot, Vitiated Coflows
Authors: Jeremy Manus, Ignacio Trueba Monje, Jeffrey Sutton
Keywords: autoigntion, most reactive mixture fraction
Abstract: The current study focuses on characterizing the auto-ignition process from turbulent fuel injection into a high-temperature, vitiated environment using the jet-in-hot-coflow burner configuration. High-speed (10-kHz acquisition rate) optical and laser-based diagnostics are used to identify ignition kernel formation and to determine the most probable mixture fraction and temperature conditions that directly facilitate ignition. Four operating cases are studied that present variations in coflow temperature, jet velocity, and fuel type. High-speed OH* chemiluminescence imaging is used to obtain data on the spatial position and delay time [following fuel injection] of the formation of the first auto-ignition kernels. High signal-to-noise ratios [SNR > 200] enable reliable measurements of mixture fraction at ultra-lean conditions that seemingly promote auto-ignition. A statistical characterization of the most probable mixture fraction values leading to ignition is presented.
Distribution Statement: 2-Distribution Limited to U.S. Government agencies only; report contains proprietary info
Acknowledged Federal Support: **Y**

CONFERENCE PAPERS:

Publication Type: Conference Paper or Presentation **Publication Status:** 1-Published
Conference Name: AIAA SciTech Forum
Date Received: 02-Aug-2022 Conference Date: 03-Jan-2022 Date Published: 01-Jan-2022
Conference Location: San Diego, CA
Paper Title: High-Speed Imaging and Laser Diagnostic Techniques in Auto-Igniting Environments at Atmospheric Pressure
Authors: Jeremy Manus, Ignacio Trueba Monje, Jeffrey A. Sutton
Acknowledged Federal Support: **N**

RPPR Final Report
as of 11-Aug-2022

Publication Type: Conference Paper or Presentation **Publication Status:** 1-Published
Conference Name: AIAA SciTech Forum
Date Received: 02-Aug-2022 Conference Date: 06-Jan-2020 Date Published: 01-Jan-2020
Conference Location: Orlando, FL
Paper Title: Seedless Velocimetry in a Turbulent Jet using Schlieren Imaging and a Wavelet-based Optical Flow Method
Authors: Bryan Schmidt, Wayne Page, Jeffrey Sutton
Acknowledged Federal Support: **Y**

Partners

,

I certify that the information in the report is complete and accurate:
Signature: Jeffrey A Sutton
Signature Date: 8/8/22 7:40PM

Project Summary - Grant # W911NF-18-1-0086
(Reporting Period: February 2018 – October 2021)

Vaporization, Mixing, and Ignition Dynamics in High-Pressure Evaporating and Reacting Sprays

Jeffrey A. Sutton
Department of Mechanical and Aerospace Engineering
Ohio State University, Columbus, OH 43210

Specific Objectives:

The objective of the proposed research is to investigate vaporization, gas-phase mixing, and ignition dynamics in evaporating (non-reacting) and reacting sprays at high pressures and high temperatures. State-of-the art optical and laser-based diagnostics are targeted for (i) characterizing the effects of injection (pressure, mass, and duration) and operating conditions (ambient pressure and temperature) on gas-phase mixing topology, (ii) examining CH_2O (low-temperature species) concentration fields, the correlation with the liquid spray and gas-phase mixing topology, and the dependence on injection and operating conditions, and (iii) providing new information regarding the role of low-temperature (first-stage) ignition and mixing dynamics on the onset high-temperature ignition. A major target is the measurement of a series of conditional statistics that detail the most probable mixture composition for facilitating ignition and the correlation between low-temperature species such as CH_2O and the onset of high-temperature, second-stage ignition. A research objective that manifested itself after the project initiation was the construction and implementation of a new, high-pressure, high-temperature spray and ignition facility that would greatly benefit the current and future research programs. Furthermore, additional measurements in an atmospheric ignition experiment were added to elucidate the fundamental roles of mixing and fluid turbulence on ignition kernel formation.

Some fundamental questions to be answered include:

(i) Where does vaporization occur in relation to the liquid spray plume, i.e., what is the correlation between fuel vapor (and vapor-ambient mixtures) and liquid droplet position? How does this change as a function of liquid mass injection and ambient density?

(ii) When (time following fuel injection) and where (with respect to the liquid spray plume) do lower-temperature species such as CH_2O form? What fuel vapor conditions are highly correlated with CH_2O formation?

(iii) What is the spatial structure of the CH_2O field following fuel injection and how does it evolve during the induction period leading to second-stage ignition? What is the correlation between the local CH_2O fluctuations and the equivalence ratio field?

(iv) When and where (spatial location) does second-stage ignition occur? What are the most probable mixing (local equivalence ratio) conditions supporting “hot” ignition?

(v) Does high-temperature ignition occur in regions of high CH_2O concentrations (i.e., regions of fuel pyrolysis and partial oxidation) or regions with high CH_2O gradients, indicating an importance in species transport and cool flame propagation?

Targeted Approach

- Test rigs: (*Former*) high-pressure spray facility; operating pressure up to 40 atm; ambient temperatures up to 700K. **After project initiation, the operating conditions of this facility was deemed inadequate to meet project goals.** (*Current*; *designed and constructed during project; completion in Fall 2019*) high-pressure spray facility; operating pressure up to 100 atm; ambient temperatures up to 1100K. Detailed characterization of environment (temperature and flow field uniformity; completion: April 2021)
- High-speed (50-kHz) Rayleigh scattering imaging for time-resolved gas-phase mixing measurement prior to ignition (downstream of liquid plume)
- High-speed (50-kHz) schlieren and Rayleigh scattering imaging for time-resolved gas-phase mixing measurement prior to ignition (downstream of liquid plume)
- High-speed (50-kHz) CH_2O PLIF imaging for time-resolved CH_2O measurements facilitating formation and transport of low-temperature species prior to second-stage, high-temperature ignition
- Simultaneous 50-kHz Rayleigh and CH_2O PLIF allow a determination of the time- and space-correlation between gas-phase mixing and "cool flame" chemistry prior to 2^{nd}-stage, "hot" ignition
- 50-kHz mixture fraction measurements (from Rayleigh) will be used to determine the most probable mixture fraction and mixture fraction gradients present at the onset of high-temperature ignition (simultaneous high-speed OH* will be used to denote the initial kernel formations)
- Atmospheric ignition measurements – time-resolved mixture fraction, temperature, and velocity measurements to understand fundamental roles of mixing and flow turbulence on ignition kernel formation (*added after project initiation during facility construction period*)

Relevance to Army

The DoD, and Army in particular, have a need for higher performance propulsion systems. Of specific relevance to the current research program is an improved understanding of spray vaporization dynamics, mixing, and ignition in diesel cycle engines. The current program targets novel diagnostics for an improved fundamental understanding of the governing phenomenon with a specific focus on characterizing the processes controlling ignition. Broader technical impacts include the development of a benchmark database for CFD assessment. There is a lack of quantitative, spatially and temporally resolved mixing (species and temperature) data that can be used for model assessment. With improved CFD models, there is potential for improvements in liquid-fueled combustor design, which can result in improved efficiencies. Across the DoD, the majority, if not all, energy-conversion systems use liquid fuel injection systems. The underpinning physics gained in the current program can be leveraged in other systems (i.e., UAV platforms) including continuously operating gas turbine engines operating on aviation fuels. Finally, it is noted that the commercial transportation sector, including heavy-duty diesel platforms, is the largest consumer of fuel resources. An improved understanding of spray dynamics and injection can be utilized for commercial technology improvements.

Results and Accomplishments

Design and Construction of New Test Facility

At the initiation of the project, the original high-pressure/temperature vessel (HPTV) described within the grant proposal was repaired and tested for operability at elevated temperature and pressure. Evaluation of capabilities led to the determination that achievable operating conditions (700 K; 30 atm) would not meet current (and future) project goals. Specifically, the upper limits of the testing conditions were the lower

bounds of the desired test matrix. Thus, in consultation with the program manager, we decided to abandon the original test rig and design and fabricate a new high-pressure/temperature system. While not an original task, this activity took substantial time that ultimately caused several project delays as described below.

A collaboration with CMT Motores (Valencia, Spain) was initiated to design a new vessel that would allow operating conditions applicable to current and future diesel (and other) engines. The design is similar to other research vessels, commonly referred to as "Aachen vessels" from Germany. The new OSU high-pressure and temperature combustion facility (HPTCF) allows optical access from four sides, with an orthogonal injector for unobstructed access for several laser diagnostic approaches. This aspect is rather unique to these types of facilities. The new HPTCF allows operation up to 100 atm and 1100K ambient conditions. Figure 1 shows photographs of the constructed vessel and its integration into our laboratory.

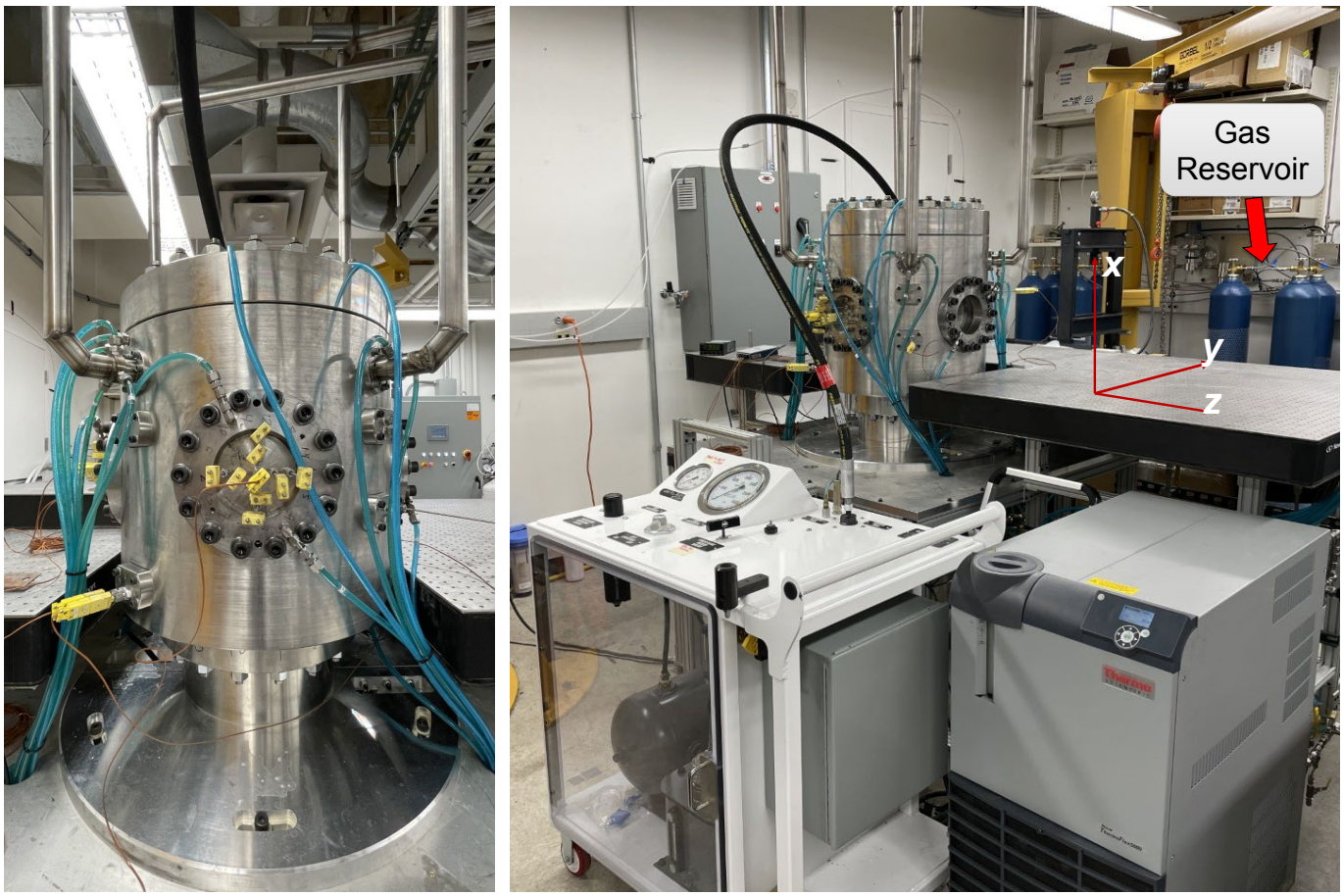

Fig. 1: (Left) Photograph of newly constructed HPTV shown with water cooling and thermocouple array. (Right) Photograph of HPTV integrated into the laboratory.

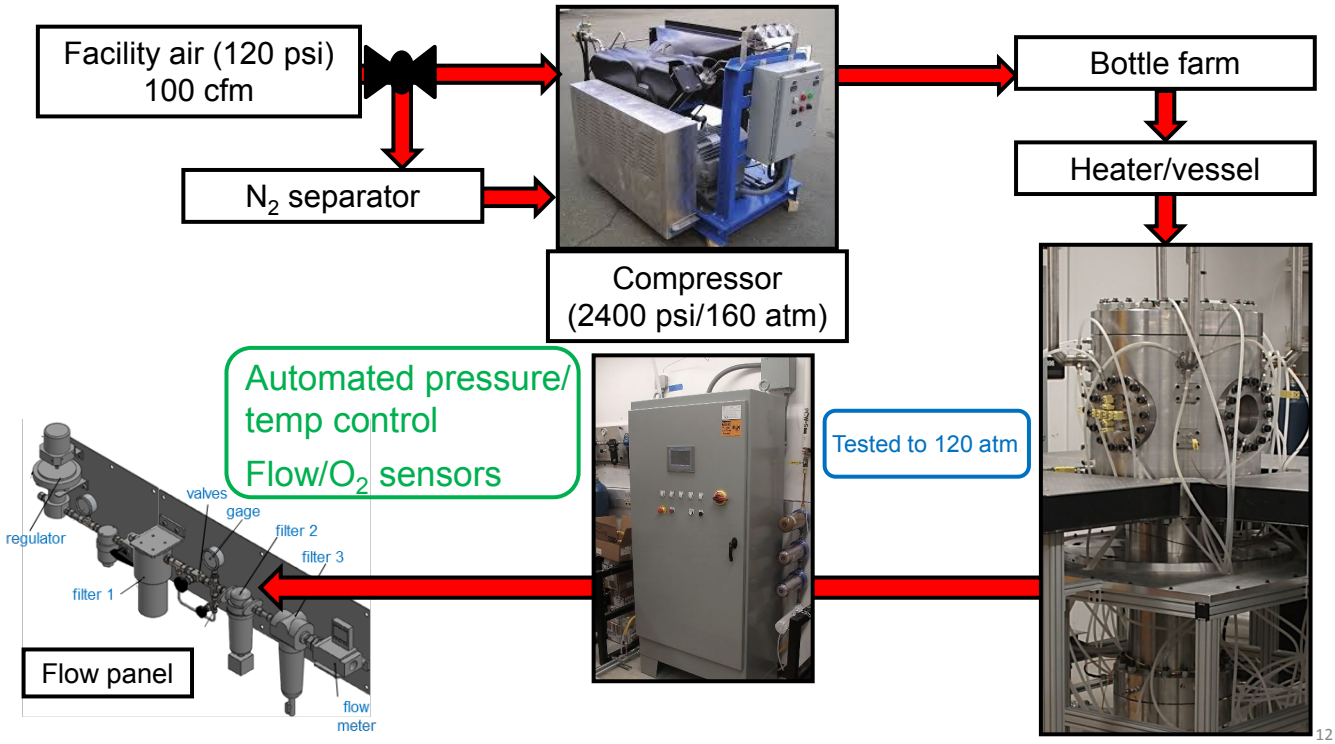

Fig. 2: (Left) Flowchart showing complete HPTCF system operation

Figure 2 shows a flowchart of the system operation of the new facility. The high-pressure vessel is integrated into a complete operational system which includes gas supply, regulation, and exhaust. Briefly stepping through the system, either air or nitrogen can be used as the test gas. Nitrogen is used for non-reacting vaporization and mixing studies and air is used in ignition and flame studies. Low-pressure compressed air (~110 psig) is routed to either (i) a nitrogen separator (removes O_2) or (ii) a bypass (for air use and combustion studies) and then the desired gas is sent directly to an air compressor that can output more than 2000 psig at 60 scfm. The compressed gas is then sent to a bottle storage facility which is connected inline to the test rig. The gas is then regulated and sent through the custom heater, the test section, and exhausted through the heat exchangers and out of the laboratory. The desired flow rates, gas temperature, and operational pressure are controlled by a master PLC control system that monitors and regulates the mass flow controllers, pressure regulator, and thermocouples/heaters. The PLC control system was custom designed for this facility and was designed to operate over a large range of thermodynamic conditions.

Testing of the facility first consisted of evaluating the temperature uniformity of the chamber under high-temperature operation. Figure 3 (left) shows results from a series of thermocouple scans. The positions of the thermocouples are denoted by the symbol location with reference to a “0” position, which is the centerline position. The false color map shows the measured temperature at that location. The right figure shows various 1D profiles at fixed positions from the fuel injector. All temperature results show that the vessel achieves very uniform temperatures at elevated temperatures. For example, the maximum deviation within the core of the vessel is less than 10K from an average temperature of 835K, which is approximately 1.2%. Figure 4 shows thermocouple-based temperature measurements as a function of distance to the water-cooled injector to characterize boundary conditions and repeatability with previous experiments in other facilities. Figure 4 demonstrates that the current measurements produce stable

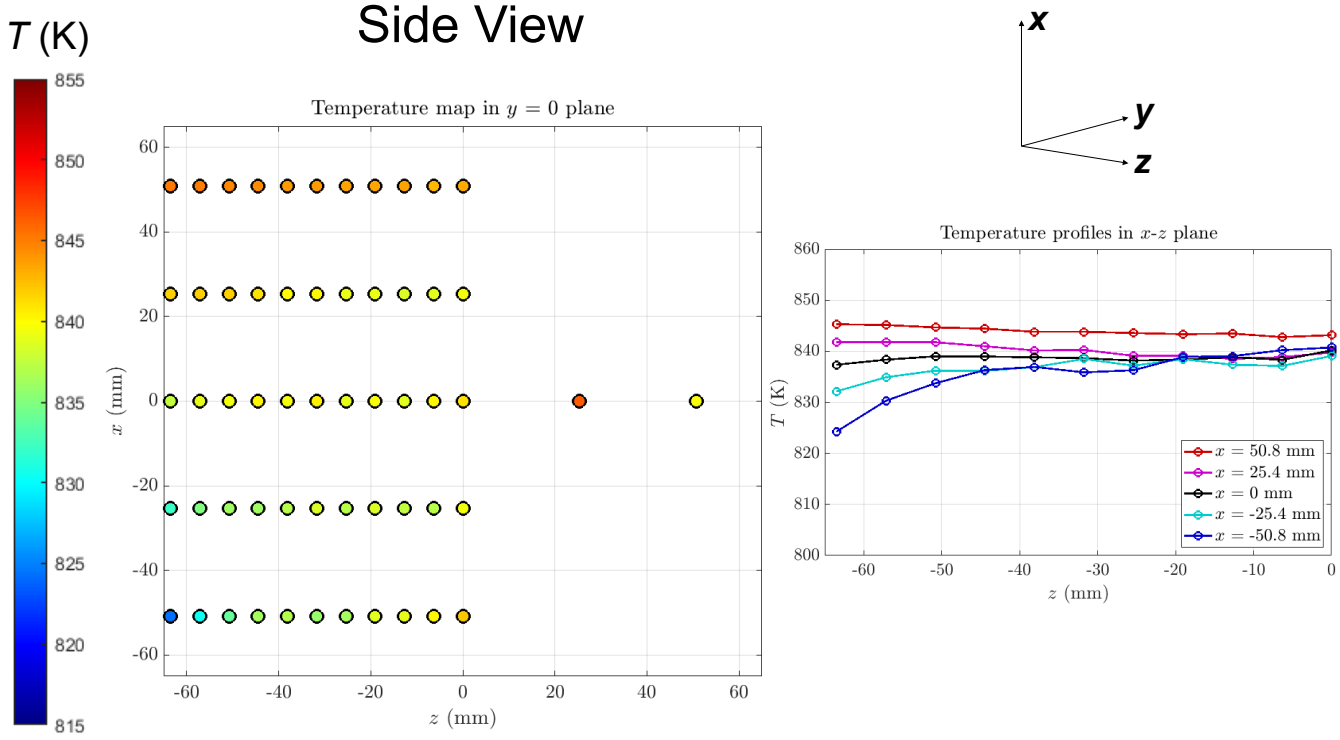

Fig. 3: (Left) Measured temperature distributions within the HPTCF. (Right) Example temperature profiles taken across the measurement domain.

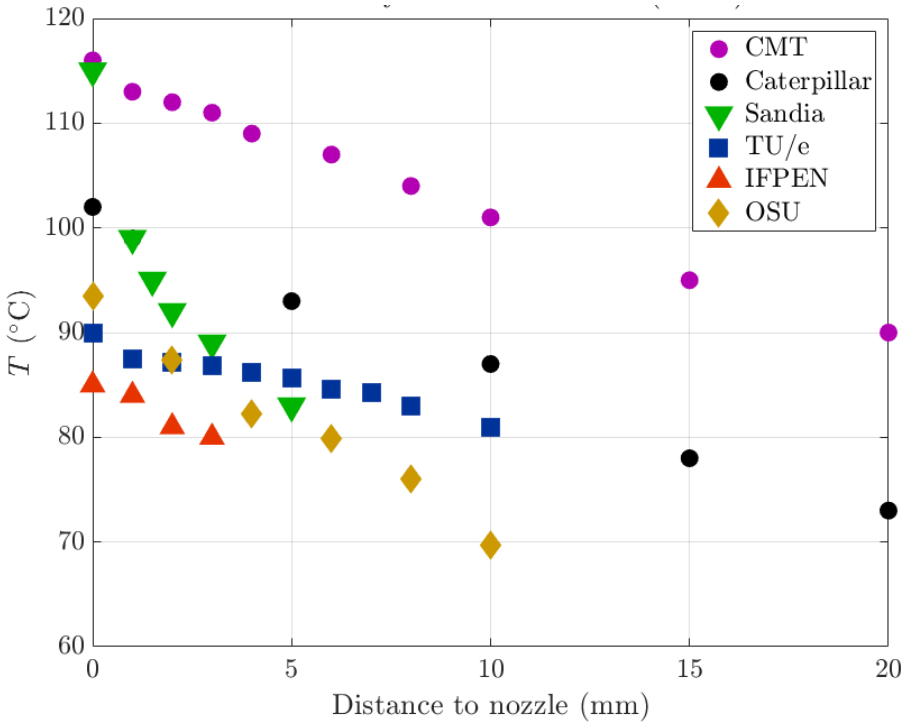

Fig. 4: Measured temperature profiles as a function of distance to injector tip. Also shown are previous measurements from Meijer et al. (2012) for comparison.

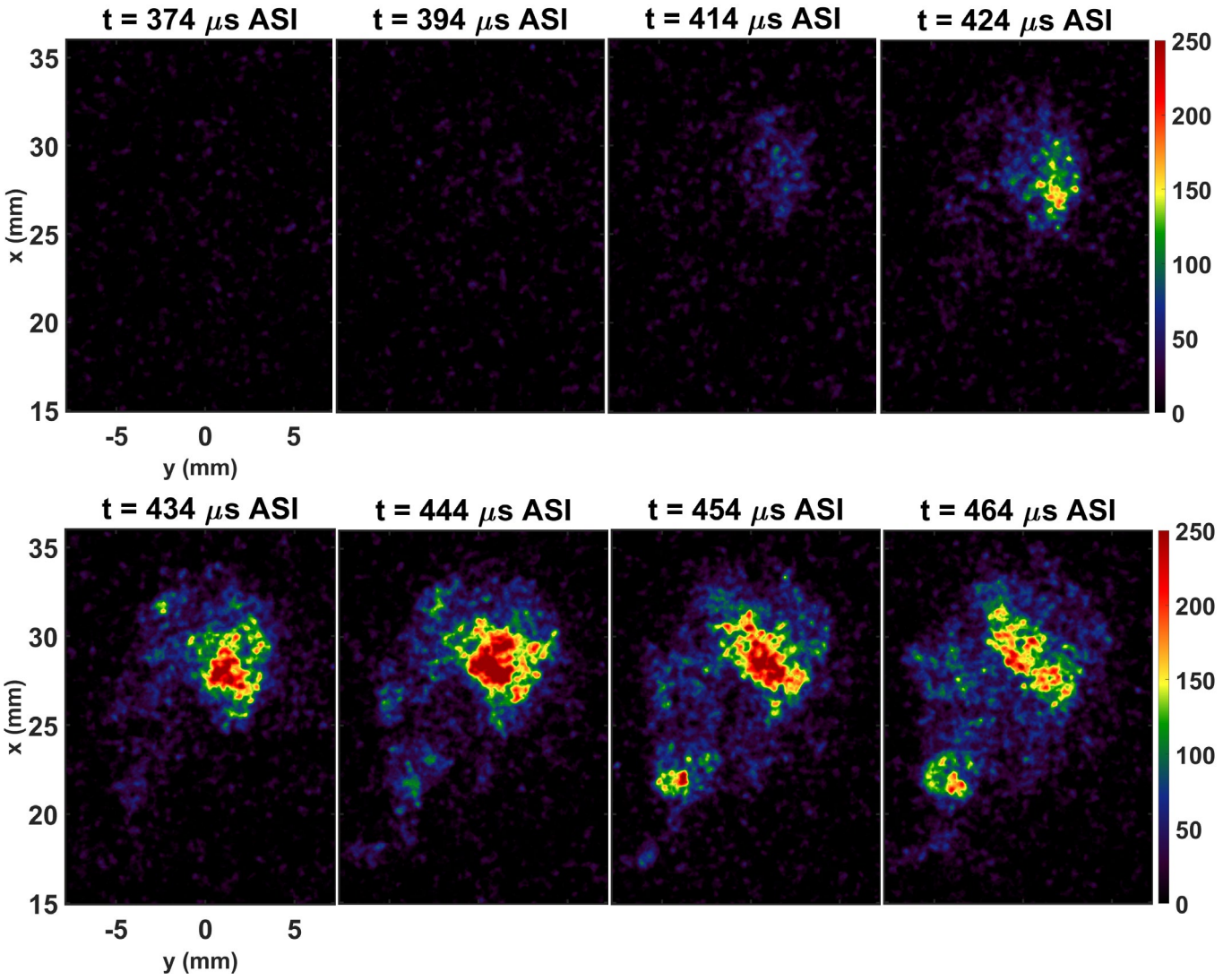

Fig. 5: Example 100-kHz OH* image sequence of $C_{12}H_{26}$ injection into 60-bar, 900-K oxidizing environment showing ignition.

injector temperatures (i.e., the facility provides sufficient cooling) that agree very well with previous measurements, thus providing a reliable environment in which to conduct testing. Finally, for reacting conditions, we tested the well-characterized Spray A conditions from the Engine Combustion Network (ECN). This consisted of injecting dodecane at 22 ksi into a 60-bar, 900-K environment of 15% O_2/85% N_2 by volume. Figure 5 shows an example ignition sequence detected by OH* chemiluminscence imaging acquired at 100 kHz. Ignition is defined to occur at the first detection of OH* (above a defined threshold). As shown in the image sequence, the first occurrence of the kernel is at 424 μs after start of injection (ASI). Previous experiments in four different and separate facilities have determined the ignition delay time to range between 410 and 440 μs ASI for Spray A conditions. Thus, the current vessel allows spray and ignition conditions that are highly repeatable and consistent with standard test facilities found within the literature. Following the detailed testing, results were presented at an ECN teleconference and were well received by the community.

Development and Optimization of Advanced Optical and Laser-Based Diagnostics

One target of the program was the measurement of gas-phase mixing in the presence of liquid-phase droplets under high-pressure conditions. Previously, we have demonstrated this capability using filtered Rayleigh scattering (FRS) diagnostics in atmospheric sprays. FRS requires the use of a detailed Rayleigh-Brillouin scattering (RBS) spectral code to analyze the results. The current RBS/FRS codes were expanded to include fuels at elevated temperature and pressure. Testing was performed to verify the accuracy of the model.

The high-energy pulse burst laser system (HEPBLS) was re-configured for simultaneous high-energy output at both 532 nm and 355 nm and successfully tested. The 532-nm output is needed for high-speed (50 kHz) Rayleigh scattering and the 355-nm output is needed for high-speed (50 kHz) CH_2O PLIF. A schematic of the re-configured HEPBLS is shown in Fig. 6a. Energy optimization results for 532-, and 355-nm output is shown in Fig. 6b. First, it is noted that the HEPBLS outputs more than 2 J/pulse at 10 kHz. We have achieved conversion efficiency of greater than 55 % at 532 nm and greater than 37.5% from the 2nd-harmonic output (532 nm) to the 3rd-harmonic output (355 nm). Next, the output energies were optimized at 50 and 100 kHz. The results are shown in Fig. 7 for 532-nm. At 10 kHz, more than 1 J/pulse is available, whereas approximately 200 mJ/pulse and 100 mJ/pulse can be achieved at 50 kHz and 100 kHz repetition rates, respectively. This confirms our previous assertions that the output energy of the HEPBLS scales with repetition rate; that is, total power is conserved regardless of laser repetition rate. In addition, this demonstrates advanced capabilities for performing high-speed laser diagnostics within the HPTCF.

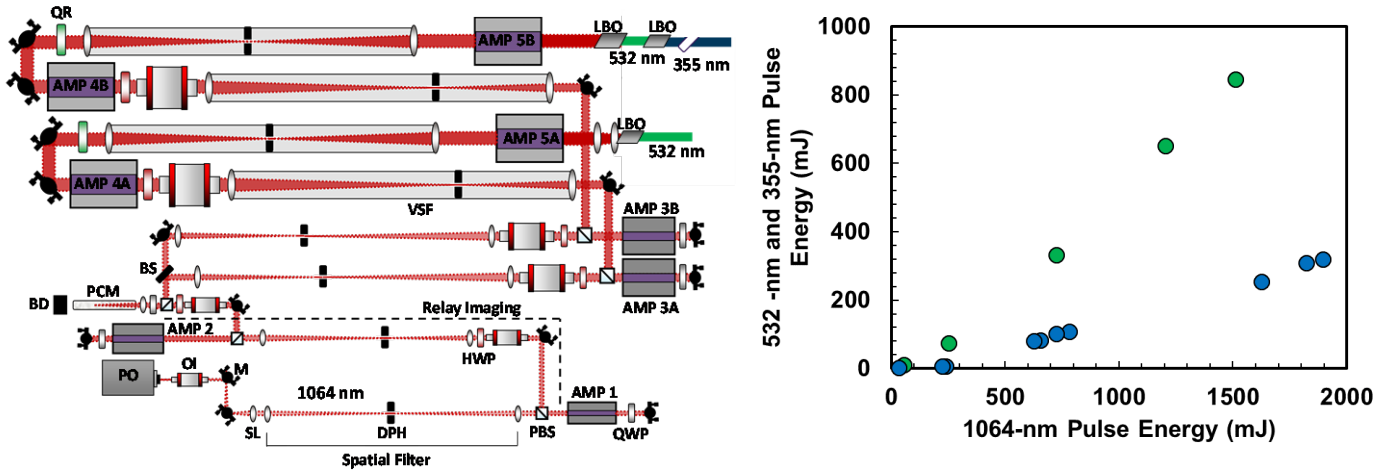

Fig. 6: (a) Schematic of high-energy, pulse burst laser system (HEPBLS). The configuration depicts 2nd-and 3rd-harmonic generation at 532 nm and 355 nm, respectively for the proposed research program. (b) Second harmonic (532 nm) and third harmonic (355 nm) output energies as a function of the fundamental 1064-nm output from the HEPBLS. Results are at 10 kHz. The 532-nm output is used for high-speed mixing (Rayleigh) measurements and the 355-nm output is used for high-speed CH_2O PLIF imaging

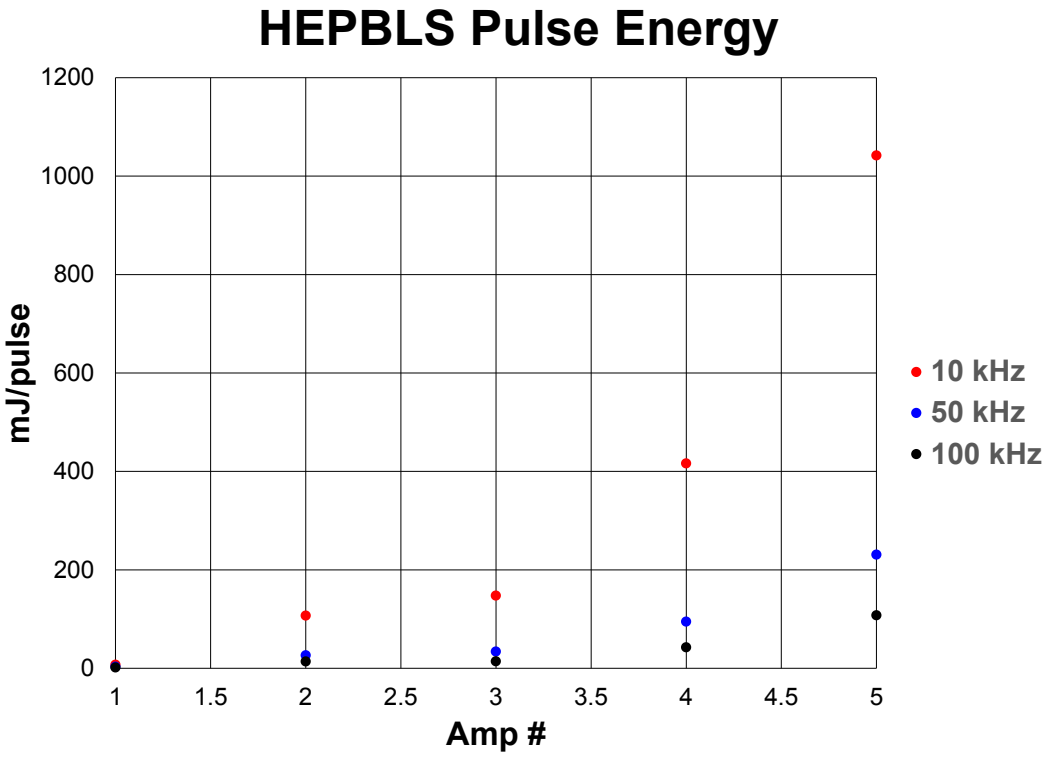

Fig. 7: Comparison of HEPBLS 532-nm output energy at 10, 50, and 100 kHz.

Measurements under High-Pressure and Temperature Conditions

Figure 8 shows an example 100-kHz schlieren image sequence within the HPTCF under Spray A conditions. The dodecane fuel is injected for 1.5 ms into a 60-bar, 900-K environment. As shown in Fig. 8, the "softening" of the schlieren image at 0.36 ms after injection signals the beginning of low-temperature heat release, followed by the onset of high-temperature, second-stage ignition at 0.44 ms ASI. The formation and growth of the ignition kernel is further tracked in time, leading to the formation of stable combustion (t > 1.1 ms ASI). Figure 9 shows measurements of fuel penetration as a function of pressure. Figure 9 shows a set of image stills extracted from 50-kHz schlieren imaging showing a comparison of fuel penetration as a function of pressure. The fuel is dodecane (a diesel surrogate) and the results show that with increasing pressure, fuel penetration is inhibited. There also is a buildup of liquid fuel at the leading edge of the fuel plume as pressure increases.

At the time of writing this report, the targeted laser-based measurements – Rayleigh scattering for mixing analysis and CH2O for low-temperature chemistry studies – have not been fully analyzed. Thus, research objectives under high-pressure operation conditions identified above (including the specific research questions) have not properly satisfied. The delay in acquiring the necessary data in the program is attributed to four major events that should be explained:

(1) At the beginning of the project, the primary post-doctoral researcher working on this project left un-expectantly. This lead to a three-month delay in activities while his replacement was found.

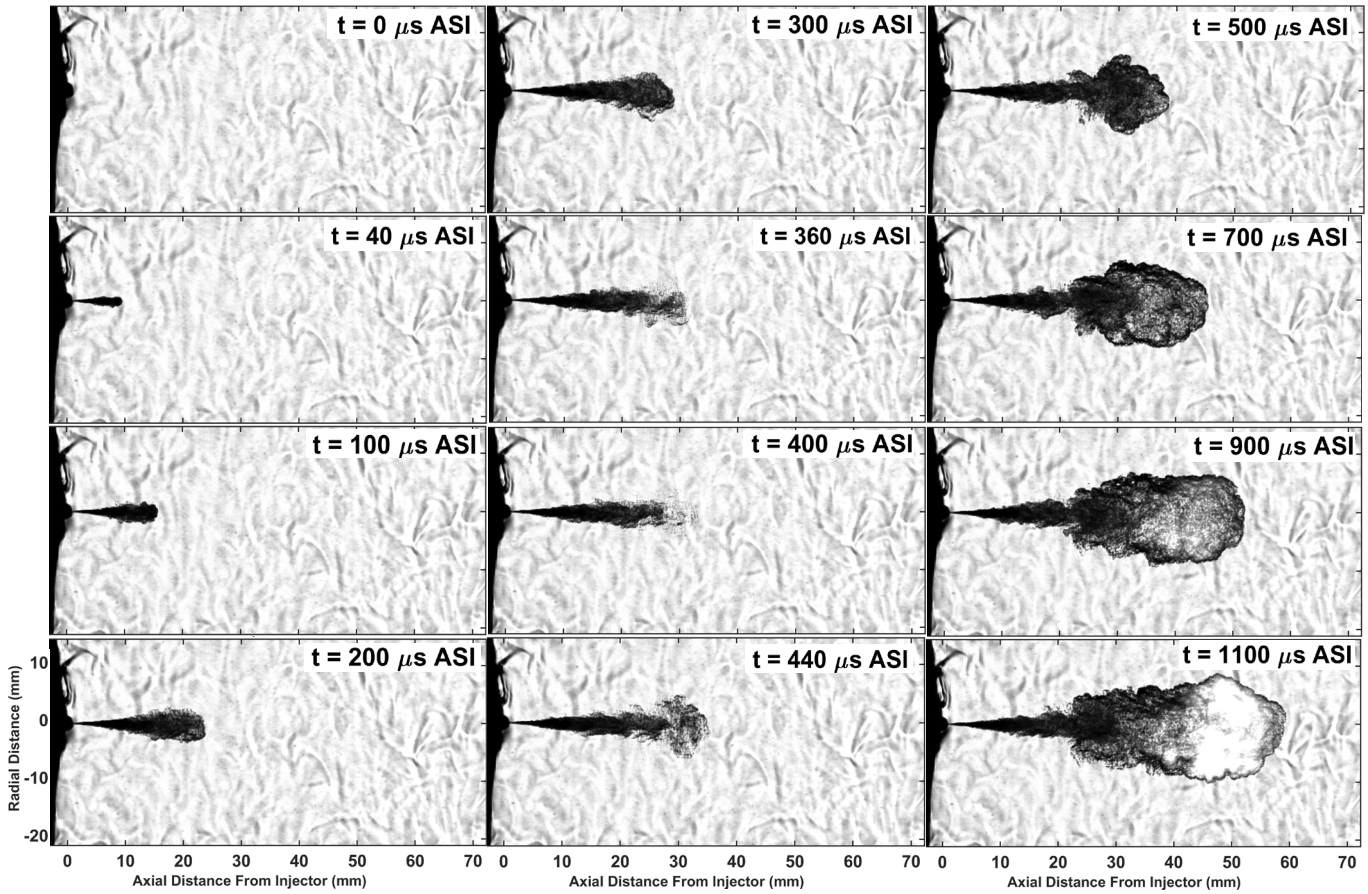

Fig. 8: Example 100-kHz schlieren image sequence showing liquid dodecane fuel injection and ignition at 60 bar, 900K.

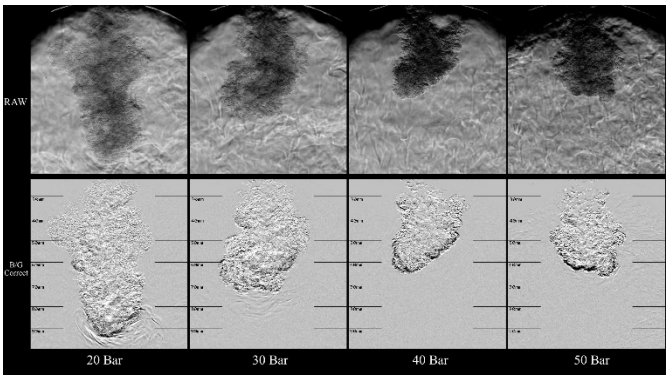

Fig. 9 – Comparison of liquid fuel penetration as a function of pressure (20 to 50 bar) for dodecane fuel.

(2) As discussed above, we decided to pursue the design and construction of a new high-pressure and temperature facility. While this facility is state-of-the-art and has allowed us to achieve much more impactful operating conditions, its design and construction did lead to a twelve-month delay.

(3) This program was undertaken during the global pandemic due to Covid-19. Our laboratories were shut down in March 2020 and re-opened on a part-time basis in July 2020 and a full-time basis in January 2021. This lead to a six-month delay.

(4) While the laboratories were closed and subsequently re-started, many major pieces of equipment did not work properly when laboratories re-opened. For example, our primary air compressor was not operational for approximately six months in 2021.

Overall, the unfortunate delays encountered within this program total to approximately 27 months. Our personnel worked tirelessly to make up a lot of the time and were granted a no-cost extension. Unfortunately, we could not make up the complete amount of time by project's end (~ 45 total months). However, we will continue to analyze the results and satisfy the bulk of the project goals after end-of-project. Discretionary funds are available to fund the graduate student who will ultimately use the data as part of his PhD dissertation. We will publish results with ARO acknowledgment.

Ignition Measurements under Atmospheric Conditions

During the HPTCF construction, we decided to develop additional tasks that would optimize project outcomes. Since we knew high-pressure experiments would be delayed, we decided to perform atmospheric ignition experiments to understand the most probable mixing, temperature, vorticity, and strain rates occurring at ignition. These measurements are of significant interest to the combustion community to provide new insights on what conditions facilitate ignition under turbulent fuel injection into high-temperature environments. These measurements also are unique and provide new data for CFD model assessment.

A photograph of the Ohio State University auto-ignition burner (AIB) is shown in Fig. 10. The 200-mm-diameter brass perforated plate serves as the flame holder for a lean H_2/air flame that provides the vitiated coflow. Cold fuel (296 K) is injected through a 5.2-mm tube that is connected to a fast-actuated solenoid valve. For the current work, the valve is triggered at rates between 1/15 and 1/21 Hz and actuated for 50 ms, which is sufficient to achieve auto-ignition and a stabilized flame. The valve response time was measured to be 7.48±0.07 ms and 7.18±0.09 ms for the low and high velocity cases, respectively. The operating conditions for the current atmospheric-pressure studies are presented in Table 1. Four cases were considered using two fuels (DME and C_3H_8), two coflow temperatures, and two fuel jet exit velocities. All fuel mixtures were diluted with 75% N_2 to increase the stoichiometric mixture fraction (ξ_{ST}) and the most reactive mixture fraction (ξ_{MR}) for measurement purposes. The most reactive mixture fraction is defined from homogenous ignition calculations and corresponds to the mixing condition that has the shortest ignition delay time. For cold fuel injection into high-temperature oxidizer streams, ξ_{MR} typically corresponds to very lean conditions due to the fact that the non-linear temperature dependence of ignition reactions overcome the effect of small fuel concentration. Flow rates for all gases are monitored with calibrated mass flow controllers with a manufacturer's stated uncertainty of <1%. The coflow gas flow rates were chosen such that the velocity of the product gases (oxidizer stream for auto-ignition process) was 4 m/s. Each fuel mixture was prepared in house using a gravimetric mixing method, followed by homogenization. The fuel composition of each cylinder was measured by flowing the gas mixture through the fuel tube and performing 1D Rayleigh scattering measurements at x/D < 1, where D is the fuel tube diameter. Measured fuel mixtures were accurate to within 1% of the targeted 25:75 ratio. The temperature boundary conditions also were measured with 1D Rayleigh scattering. Temperature profiles across the coflow were uniform and were < 3.5% below the adiabatic flame temperature (see Table 1).

OH* chemiluminescence (CL) imaging is used in two capacities in the current work. First, the OH* images are used to detect the formation of the initial ignition kernels to describe the stochastic nature of the auto-ignition process in terms of ignition height and delay time probability density functions (PDFs). Second, the OH* imaging is used in conjunction with the high-speed LRS-based mixture fraction and

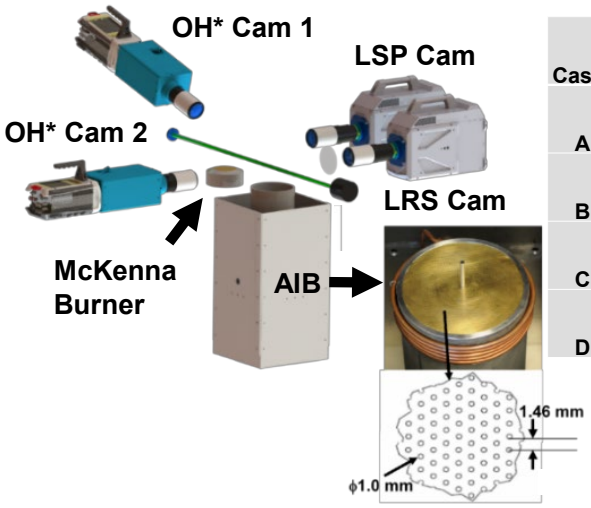

Fig. 10 – Schematic of imaging setup and photograph of autoignition burner.

Case	Fuel	Re	T_{ox} (K)	ξ_{ST}	V_{jet} (m/s)	τ_{ig}^{OH*} (ms)	H_{ig}^{OH*} (mm)
A	D-DME	13600	1328[a]	0.163	30	6.74 ± 0.49	72 ± 9.2
B	D-DME	27200	1328[a]	0.163	60	5.78 ± 0.53	78.9 ± 11.9
C	D-DME	13600	1469[b]	0.148	30	3.06 ± 0.14	53.1 ± 4.5
D	D-C_3H_8	29000	1328[a]	0.103	60	3.8 ± 0.35	57.1 ± 12.2

Table 1 – Operating conditions and global ignition statistics

temperature measurements to identify a search region for ignition detection via elevated temperatures as described below. A two-camera configuration is used to capture the OH* images - one camera oriented normal to the laser plane to determine height and transverse location and the other camera oriented parallel with the laser sheet, to identify ignition kernel formation that occurs within the thickness of the laser sheet (Fig. 10). For the global ignition statistics, all OH* images are used. For the mixture fraction/temperature measurements, only the image sequences where the first OH* kernel forms within the thickness of the laser sheet are used during analysis. The cameras are high-speed intensified CMOS cameras (Phantom V710 + LaVision HS-IRO), coupled with a 100-mm f/2.8 Cerco UV camera lens. A combination of long pass and band pass filters (WG295 and UF11) are used to capture only the OH* emission near 310 nm. The field-of-view (FOV) of the planar OH* camera was 82 mm x 63 mm with a projected pixel size of ~103 µm and the FOV of the 'top-down' OH* camera was 98 mm x 63 mm with a projected pixel size of ~122 µm. An imaging processing algorithm was developed for determining the first ignition kernel (defined by OH*) based on area and intensity thresholds. The ignition height (H_{ig}^{OH*}) is determined as the centroid of the area of the detected OH* kernel and the ignition delay time (τ_{ig}^{OH*}) is defined as the time between the fuel exiting the tube and the OH* kernel detection.

Laser Rayleigh scattering (LRS) is performed to provide measurements of temperature and mixture fraction prior to and at the onset of auto-ignition. The high-energy pulse burst laser system (HEPBLS) is used for the high-speed LRS measurements. For the current measurements, the HEPBLS was operated with a 532-nm output energy of approximately 900 mJ/ pulse at 10 kHz and a burst duration of up to 11 ms. The laser beam was first expanded through a cylindrical telescope using a combination of f = -300 mm and a f = 750 mm cylindrical lenses and then focused over the burner using an f = 750 mm cylindrical lens to form a laser sheet that is 28 mm tall with a measured sheet thickness of < 250 µm. The optical set-up (Fig. 10) consisted of both a planar LRS camera and laser sheet profiling (LSP) camera, both of which were high-speed Photron SA-Z CMOS cameras. The LSP Cam images a region of uniform air issuing from a matrix (McKenna) burner and is used to correct the LRS measurements for shot-to-shot laser intensity fluctuations (and sheet non-uniformities). The light collection is optimized using a combination of an achromat and an f/1.4, 85-mm camera lens, leading to a magnification of 0.35 and projected pixel size of ~56 µm.

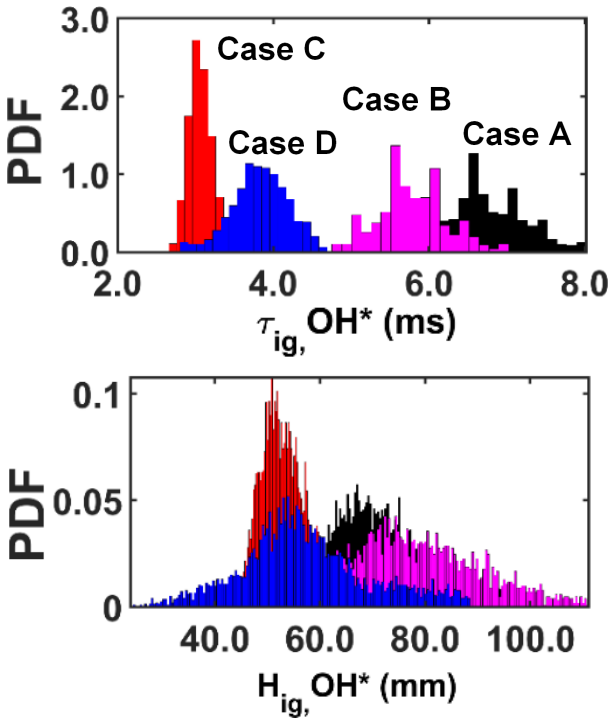

Fig. 11 – PDFs of (a) ignition delay time and (b) ignition height for all kernels detected using OH* CL.

To resolve mixture fraction at conditions very lean conditions ($\xi << \xi_{ST}$), it is crucial to have high measurement precision which can be cast in terms of a signal-to-noise ratio (SNR). A set of carefully selected image processing methods were utilized to increase image SNR without removing relevant spatial frequencies. First, each raw image was darkfield corrected to account for sensor offset and sensor non-uniformity was corrected. Second, each image was corrected for the non-uniform laser sheet intensity profile using the LSP Cam. Third, image artifacts due to refractive index gradients were removed. Finally, a de-noising method was applied to the images using biorthogonal wavelets that properly preserves high-frequency content. The SNR is defined in two ways in this work to characterize measurement precision. Using a 50-column region in the coflow, the ratio of the mean temperature to its standard deviation is defined as the "spatial" signal-to-noise ratio, SNR_S, and was found to vary between 250 and 600 for all images. Second, the fluctuations between the derived mean coflow temperature for each laser pulse within a burst are used to derive the "intra-burst signal-to-noise" or SNR_B. Figure 2 shows example intra-burst temperature records for all four cases. For all cases, the average value of $SNR_B > 200$ and sets the limiting minimal detectable ξ value as $1/ <SNR_B> \approx 0.005$.

Probability density functions (PDFs) of ignition delay time, τ_{ig}^{OH*}, and ignition height, H_{ig}^{OH*}, are shown in Fig. 11 and the mean values (M) and standard deviations (σ) are displayed in Table 1 in the form of M ± σ. As expected, the highest coflow temperature case (C) has the shortest ignition delay time, lowest ignition height, and smallest standard deviations of both metrics. Consistent with previous work], the higher temperature coflow conditions lead to reduced variability in ignition location and delay time. A comparison between Case B and Case D allows a look at the effect of fuel (D-DME vs D-C_3H_8) for equivalent temperature and exit velocity (and nearly equivalent Reynolds number). There is a significant fuel effect as the mean ignition height and time of D-DME fuel are greater than that of the D-C_3H_8 fuel by 50% and 40%, respectively. Comparing Case A to Case B allows insight into the effect of changing exit velocity (and hence bulk fluid residence time and global strain rate). While there are differences between the two cases, the effect of jet exit velocity on ignition statistics appears much smaller than that of temperature or fuel type for the cases considered. With a factor of two increase in exit velocity, the mean ignition time and height decrease by 15% and 10%, respectively. The opposite trends between ignition height and delay time may be explained by the competing effects of increasing convective velocity ($H_{ig}^{OH*} \uparrow$) and increasing mixing due to increased turbulence intensity ($\tau_{ig}^{OH*} \downarrow$).

To characterize the most probable set of mixture fraction values that facilitate ignition, an ignition event is defined by a temperature rise due to the fact that this occurs prior to the occurrence of OH* as shown below. The OH* images (where the first occurrence forms within the LRS laser sheet) are used to identify a search window that is applied to the ξ and T fields. Using the coflow temperature record for all bursts for given case, the mean coflow temperature and standard deviation, σ, are determined. Within the defined search region, an initial temperature rise is set as $\Delta T_{ig,1} = 3\sigma$. Temperature contours 3σ away from the mean ($T_{ox} + \Delta T_{ig,1}$) are located and tracked back in previous frames as far as possible. The 3σ

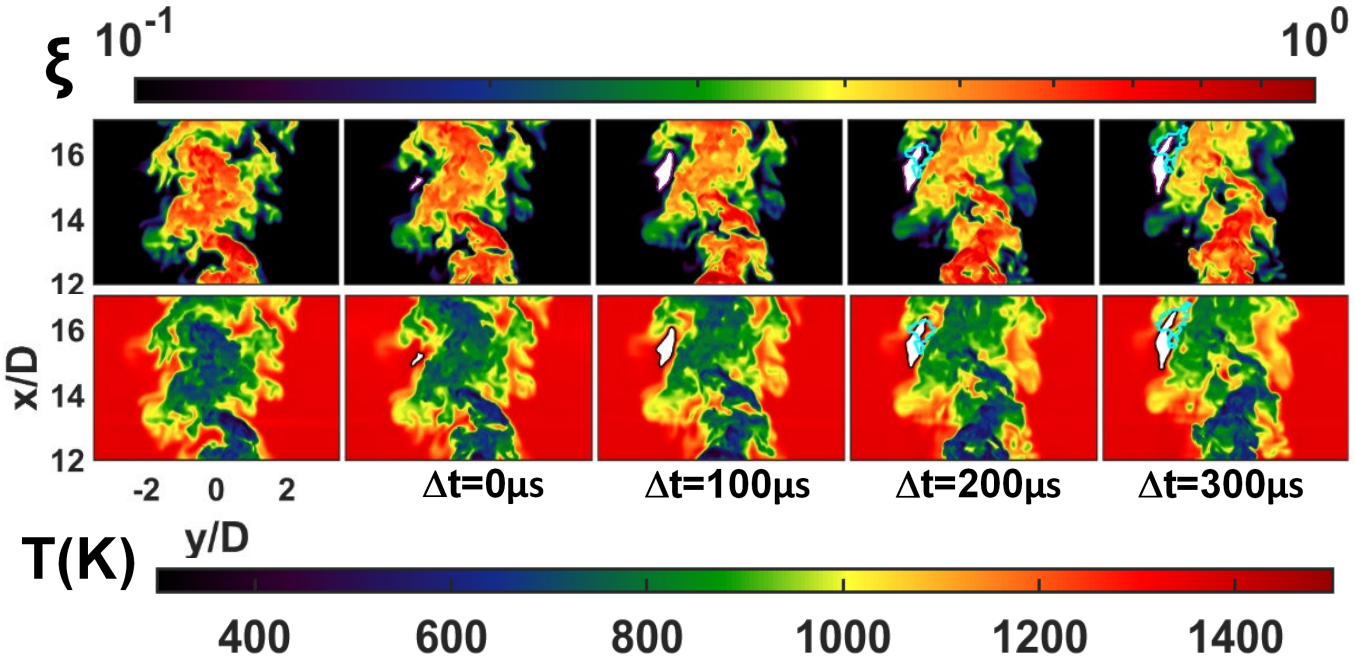

Fig. 12 – Example 10-kHz image sequence of mixture fraction (top) and temperature (bottom) fields during the first 300 μs of an auto-ignition event for Case A. The white contoured region represents the ignition kernel based on a defined temperature rise and the cyan iso-contour line represents the occurrence and growth of the OH* kernel.

threshold is used to ensure that > 99.6% of non-reacting coflow samples are not mis-identified as ignition due to uncertainty. False identification of a temperature rise due to ignition is practically eliminated by further enforcing a contour area threshold of 75 pixel^2. Next, a refinement step is introduced; that is, a second search region is defined within the $T_{ox} + \Delta T_{ig,1}$ temperature contour, and a new threshold, $\Delta T_{ig,2} = 2\sigma$ is set and the contour area threshold is reduced to 50 pixel^2. Once the $T_{ox} + \Delta T_{ig,2}$ temperature contours are identified, they are again tracked back in previous frames as far as possible, and the earliest occurrence is denoted as the initial ignition kernel (at time τ_{ig}^{RAY}).

Figure 12 shows an example image sequence of the mixture fraction and temperature fields during the formation and evolution of one ignition kernel. Here, Δt=0 μs represents the first occurrence of the ignition kernel, shown by the solid white region, followed by 300μs of growth. The cyan contours show the outline first OH* kernel. In this example, it is apparent that the first kernel detected using a temperature rise occurs approximately 200 μs earlier than the initial detection of an OH* kernel. Upon examining the image sequence shown in Fig. 12, it is apparent that the ignition event occurred in the jet periphery under lean mixture fraction conditions. Additional examples for each case are shown in Fig. 13, where the white contour represents ξ_{ST} and the cyan contour represents ξ_{MR}. These examples highlight that the kernel does appear to form near ξ_{MR}. However, because the mixture fraction gradients are so large near the kernel, the region encompassed by the kernel area corresponds to a range of mixture fraction values apparently bounded by $0 < \xi_{ig} < \xi_{ST}$.

PDFs of the most probable mixture fraction at ignition, ξ_{ig} are shown in Fig. 14 for all cases using two different detection methods. Figure 8a and 8b show the PDFs calculated using detection Method 1 and detection Method 2, respectively. The PDFs are generated from 185, 90, 210, and 80 separate ignition events for Cases A-D, respectively. The symbols correspond to the discrete PDF, while the solid lines correspond to exponential fits through the PDFs. For reference, the values of ξ_{MR} for Cases A-D are indicated with dashed lines. For the results shown in Fig. 14, any value of detected mixture fraction less

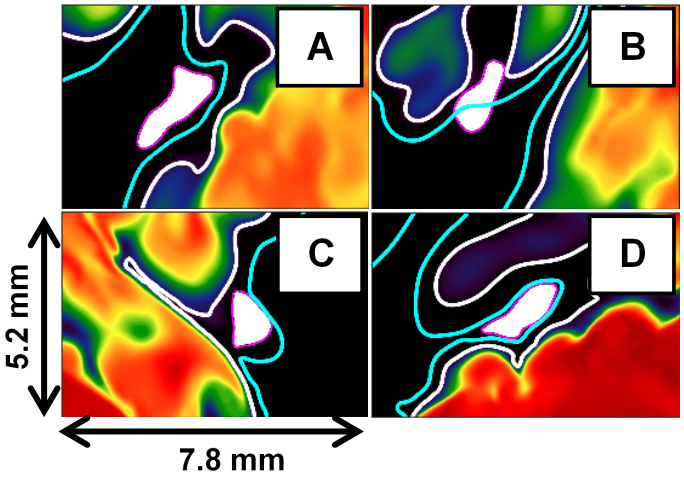

Fig. 13 – Zoomed in" view of the mixture fraction fields at the time of kernel detection. The white and cyan lines represent the ξ_{ST} and ξ_{MR} contours, respectively. The colormap is repeated from Fig. 12.

than the measurement resolution ($\xi < 0.005$) are not included in the PDFs. These values could be real, ultra-lean samples or small, undetected reacted regions with elevated temperatures (yields non-physical $\xi < 0$ values based on binary mixing-based processing). For all cases, mixture fraction values near ξ_{MR} are preferentially encountered, but the PDFs demonstrate variability in the values of ξ_{ig}, as the PDFs appear to be described by an exponential decay. In fact, ξ_{ig} values span the full range of flammability limits, although the probability for rich values is very small. It is noted that if the cumulative density function is generated from the PDFs, it is found that the majority of the detected samples occur for values of $\xi_{ig} < \xi_{ST}$, demonstrating the preponderance for lean ignition. Using detection Method 2 (as an example), the mean values of ξ_{ig} for Cases A-D are 0.03, 0.05, 0.08, and 0.01, which are in agreement with the values of ξ_{MR} determined from the homogenous ignition calculations. For all cases, the PDFs exhibit a tail that extends into rich mixture fraction values. Further improvements to the ξ_{ig} detection methods are needed to discern the extent in which ξ_{ig} varies over a large number of ignition events. Even with the current uncertainties in the quantitative nature of the PDFs, they provide evidence to show that the most probable values of ξ_{ig} are lean and likely distributed around ξ_{MR}.

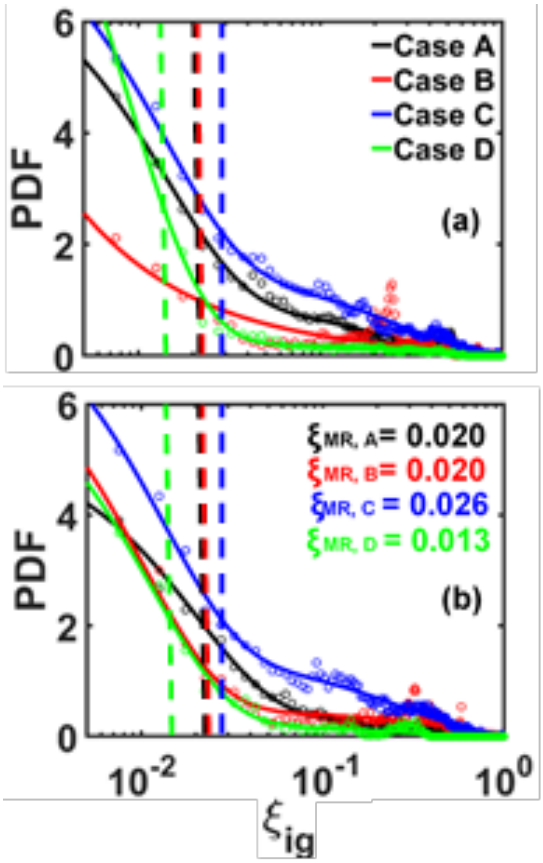

Fig. 1 – PDFs of ξ_{ig} found using (a) Method 1 and (b) Method 2. Dashed lines correspond to ξ_{MR} values

Summary - Overall, transient fuel injection of a cold turbulent fuel jet and the subsequent auto-ignition process was studied using a JHC configuration and high-speed optical and laser-based imaging. Four cases were examined that had variations in coflow temperature, fuel jet velocity, and fuel type. Global ignition statistics showed that the ignition delay times and heights displayed a strong sensitivity to temperature and fuel type, but displayed a weaker dependence on fuel jet velocity. High-resolution, kHz-rate laser Rayleigh scattering (LRS) was used to provide simultaneous mixture fraction and temperature measurements prior to and at the onset of ignition. The measurements resolved the smallest spatial scales and exhibited an SNR > 200, which permitted detection of ultra-lean mixture fraction values. PDFs of the most probable mixture fraction values at ignition are presented and compared with calculated values of ξ_{MR}. The results show that lean conditions near ξ_{MR} are preferentially encountered and the average values of ξ_{ig} agree reasonably well with the calculated values of ξ_{MR} for each case. The PDFs are characterized by a near-exponential distribution, with a finite number of rich ignition samples. At this point, it is unknown whether these are realistic or a consequence of the limitations to the current detection methods.